

1 **Salpyran: A Cu(II) Selective Chelator with Therapeutic Potential**

2 Jack Devonport, Nikolett Bodnár, Andrew McGown, Mahmoud Bukar Maina, Louise C. Serpell,

3 Csilla Kállay,* John Spencer,* and George E. Kostakis*

Cite This: <https://doi.org/10.1021/acs.inorgchem.1c01912>

Read Online

ACCESS |



Metrics & More

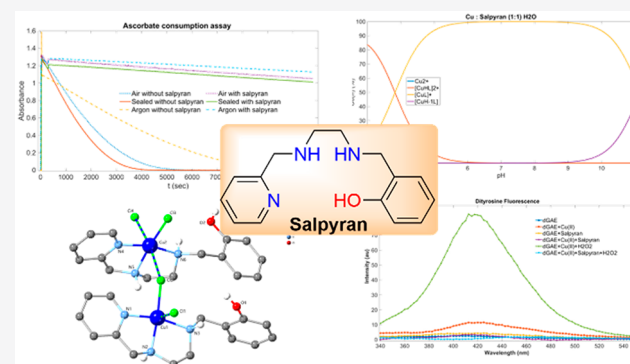


Article Recommendations



Supporting Information

4 **ABSTRACT:** We report the rational design of a tunable Cu(II)
 5 chelating scaffold, 2-(((2-((pyridin-2-ylmethyl)amino)ethyl)-
 6 amino)methyl)phenol, **Salpyran**. This tetradentate (3N,1O) ligand
 7 is predicated to have suitable permeation, has an extremely high
 8 affinity for Cu compared to clioquinol ($pCu_{7.4} = 10.65$ vs 5.91), and
 9 exhibits excellent selectivity for Cu(II) over Zn(II) in aqueous
 10 media. Solid and solution studies corroborate the formation of a
 11 stable $[Cu(II)(3N,1O)]^+$ monocationic species at physiological pH
 12 values (7.4). Its action as an antioxidant was tested in ascorbate, tau,
 13 and human prion protein assays, which reveal that **Salpyran** prevents
 14 the formation of reactive oxygen species from the binary Cu(II)/
 15 H_2O_2 system, demonstrating its potential use as a therapeutic small
 16 molecule metal chelator.

17 **INTRODUCTION**

18 The dysregulation and accumulation of biometals is a common
 19 pathological hallmark of many neurodegenerative disorders,
 20 such as Alzheimer's (AD), Parkinson's (PD) and prion
 21 diseases.^{1–9} AD is the most prevalent adult neurodegenerative
 22 disorder and the most significant cause of dementia.^{10,11}
 23 Currently, 24 million people suffer globally, and, with an aging
 24 population, this figure may double by 2040.^{12,13} AD is
 25 characterized by intracellular accumulation of neurofibrillary
 26 tangles formed of misfolded tau proteins and the extracellular
 27 deposition of fibrillar amyloid- β ($A\beta$) peptides. However, AD
 28 is a multiparameter disease, and other factors contribute to its
 29 etiology such as mitochondrial dysfunction, genetics, and
 30 age.¹⁴ At present, a large body of research suggests that metal
 31 ion dyshomeostasis plays a role in AD's pathology; therefore,
 32 the restoration of biometal homeostasis offers a new clinical
 33 target when developing AD therapies.^{6,15–22}
 34 Recent trends show that drug development into disease-
 35 modifying therapies (DMTs) for AD is broadening its scope
 36 beyond the classical primary targets of $A\beta$ and tau
 37 aggregation.^{23,24} A paucity of new treatments for AD, for
 38 almost two decades, and the low success rate of drugs in
 39 clinical trials have furthered the need to widen the scope of
 40 both targets and approaches in curbing disease progres-
 41 sion.^{25,26} Recently, the first DMT (aducanumab) was approved
 42 by the Food and Drug Administration (FDA) for the treatment
 43 of AD patients. By targeting the production and aggregation of
 44 $A\beta$, this novel therapy was found to reduce senile plaques,
 45 although there still remains some uncertainty in its clinical
 46 benefits.

47 Metal ions can affect the self-assembly of amyloid proteins;
 48 for example, $A\beta$ has a picomolar affinity for Cu(II) binding via
 49 histidine binding.^{27,28} Cu(II) imbalances exist in AD affected
 50 brains, and Cu(II) can be found either upregulated or
 51 downregulated depending on the locality of the tissue.^{6,29}
 52 Due to its redox potential when bound to $A\beta$, Cu(II)
 53 contributes to the generation of reactive oxygen species
 54 (ROS), leading to oxidative neuronal damage.^{30–32}

55 In the past decade, there has been an increasing interest in
 56 designing Cu-specific small molecule metal chelators
 57 (SMMCs) aiming to reduce Cu(II)- $A\beta$ induced oxidative
 58 stress and the resulting pathogenic consequen-
 59 ces.^{6,15,34–39,16–22,33} Chelation therapy aims to disrupt
 60 potential toxic interactions of metal ions and biomolecules
 61 by targeting specific metal ions and promoting redistribution
 62 or excretion. When designing a Cu-specific SMMC, both the
 63 thermodynamic properties of the metal chelate and the
 64 pharmacological properties of the ligand must be considered.
 65 The key criteria for Cu(II) targeting AD therapeutic are
 66 denticity, metal/ligand stoichiometry, and the coordination
 67 environment and geometry of the complex at physiological pH
 68 values. Ideally, the given ligand would coordinate to Cu(II) in
 69 a 1:1 stoichiometry, as ligands of this type exhibit a higher
 70 copper affinity than similar 1:2 complexes due to the

Received: June 24, 2021

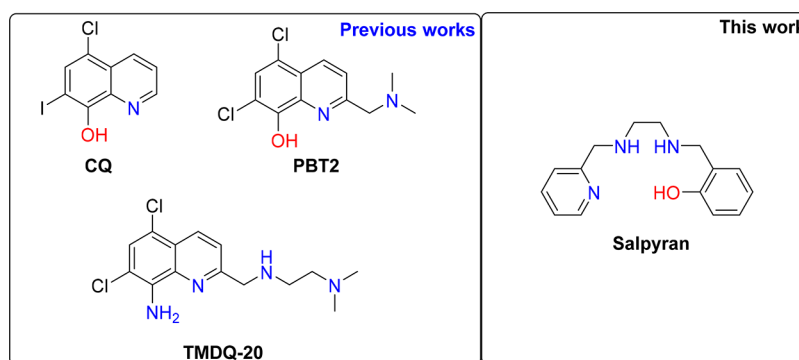


Figure 1. Previous and current SMMCs 2-(((2-((pyridin-2-ylmethyl)amino)ethyl)amino)methyl)phenol, **Salpyran**.

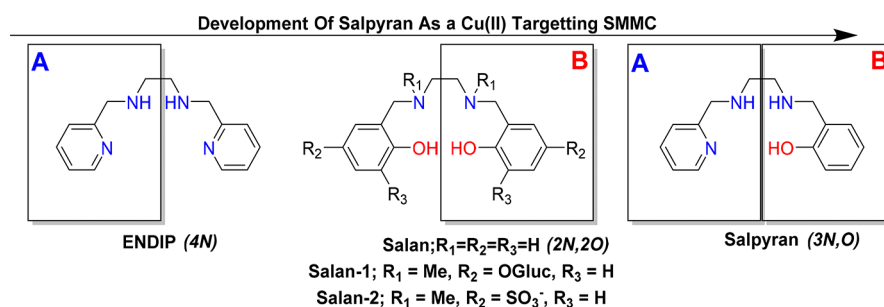


Figure 2. Development of **Salpyran** by combining structures of **ENDIP** and **Salan**.

71 chelation.⁴⁰ The increased shielding observed in 1:1 complexes
 72 protects the metal ion from the physiological environment,
 73 preventing further biological interactions such as the formation
 74 of $[A\beta(Cu)L]$ ternary species.^{39,41} Also, to be an effective
 75 therapeutic, both the ligand and the formed metal complex
 76 must be metabolically stable, nontoxic, and possess suitable
 77 aqueous solubility. Moreover, to be effective in AD, the
 78 SMMC should be able to pass through the blood–brain barrier
 79 (BBB) to reach the site of Cu(II) accumulation. For passive
 80 diffusion, this requires a SMMC that is suitably hydrophobic to
 81 passively pass through the membrane yet hydrophilic enough
 82 to stay soluble in physiological environments.^{42,43}

83 Clioquinol (**CQ**, Figure 1) was investigated in phase II
 84 clinical trials for targeting metal homeostasis as an AD
 85 treatment. **CQ** is a bidentate ligand that forms a $[Cu(II)L_2]$
 86 complex with an 2N,2O coordination environment. By
 87 targeting both Cu(II) and Zn(II) binding, **CQ** showed some
 88 improvements in the cognition of the patients trialed.⁴⁴
 89 However, due to neurotoxic side effects, the clinical progress of
 90 **CQ** was ultimately abandoned.⁴⁵ This led to the design of a
 91 second-generation tridentate 5,7-dichloro-2-
 92 ((dimethylamino)methyl)quinolin-8-ol (**PBT2**, Figure 1),
 93 which completed Phase II clinical trials.^{46,47} Introduction of
 94 a dimethylamino unit at the C2 position introduced a new
 95 binding site, but still $[Cu(II)L_2]$ complexes are formed.⁴⁸ A
 96 lack of reduction in amyloid plaque levels in the brains of AD
 97 patients and only mild cognitive benefits mean that **PBT2** has
 98 not progressed into more extensive clinical studies. The poor
 99 metal selectivity is a possible reason for the clinical failure of
 100 **CQ**, as interactions with other biometals or metalloproteins/
 101 substrates *in vivo* are conceivable. The formation of the
 102 $[Cu(II)L_2]$ species, in both **CQ** and **PBT2** cases, speculates
 103 the likely *in vivo* formation of ternary $L(Cu)A\beta$ species that
 104 can contribute to increased ROS production.⁴⁹

Due to the clinical potential demonstrated by **CQ** and
PBT2, several tetradentate ligands based on similar scaffolds
 have been developed to increase Cu(II) selectivity and
 minimize unwanted biological interactions.^{38,40,48,50,51} This
 incremental design led to the state-of-art Cu(II) chelator,
TDMQ-20 (Figure 1).⁵² **TDMQ-20** is an 8-aminoquinoline
 derivative that offers a 4N coordination environment and
 shows exceptional selectivity for Cu(II) ions. Recently,
TMDQ20 has been studied as an AD therapeutic in early
 stage nontransgenic mouse models and late-stage transgenic
 models.⁵² Oral treatment offered significant improvements in
 both the behavioral and cognitive impairments observed in
 each model, while also reducing oxidative stress in the mouse
 cortices. This efficacy paves the way for future pharmacological
 evaluation of SMMCs; thus, most research heavily focuses on
 chelators based around either 8-hydroxy/8-amino quinoline
 backbones. Having the chemical criteria and fall-outs from
 previous studies in mind,³⁹ and aiming to develop new
 chelators not derived from 8-hydroxy/8-amino quinoline cores,
 we hypothesized that the scaffold 2-(((2-((pyridin-2-
 ylmethyl)amino)ethyl)amino)methyl)phenol, **Salpyran** (Fig-
 ure 1) would be an ideal therapeutic Cu(II) targeting SMMC.
 Herein, we report the criteria considered in designing
Salpyran, its synthesis and characterization, solid-state and
 solution studies, and ROS inhibition.

RESULTS AND DISCUSSION

Scaffold Development. Several organic ligands, exclusive
 of hydroxy and aminoquinolines frameworks, have been
 investigated as potential Cu(II) SMMCs. A recent review by
 Hureau et al. highlights the pros and cons of these structures.³⁹
 Among them, tetradentate bis(pyridine), **ENDIP**, competes
 for both copper and zinc in $A\beta$ aggregates, preventing their
 formation and solubilizing amyloid precipitates.⁵³ Tetrahy-
 drosalen (**Salan**) ligands are strong metal binders and offer

Table 1. Thermodynamic and Calculated Pharmacological Relevant Properties of Chelators Targeting Cu(II) Homeostasis in Alzheimer's Disease*

| | Thermodynamics | | | | | Drug Likeness ^[f] | | | | | | | |
|----------|----------------------|---------------------|----------------------|-----------|---|------------------------------|----------|--------|--------|------|-----------|------------|-------------|
| | pCu ^[a] | pZn ^[a] | Cu/Zn ^[d] | M/L ratio | Cu(II) Coordination Environment ^[c] | Mw (g/mol) | TPSA (Å) | cLog P | cLog S | HB D | BBB Perm. | GI Absorp. | Ref. |
| Cu(Aβ) | 7.3-7.8 | ~6.0 | ~ | - | HisN ₃ Glu11/Aps ¹ O H ₂ O _{ap} | - | - | - | - | - | - | - | 39,65,75,76 |
| CQ | 5.91 ^[b] | 5.64 ^[b] | 0.27 | 1:2 | N ₂ O _{2eq} | 305.5 | 33.12 | 2.96 | -4.37 | 1 | Yes | High | 77-79 |
| PBT2 | n.d | n.d | n.d | 2:1 | N ₃ O ₂ | 271.14 | 36.36 | 2.85 | -3.98 | 1 | Yes | High | 48 |
| TMDQ-22 | 10.75 ^[c] | 5.06 ^[c] | 5.69 | 1:1 | N _{4eq} Cl _{ap} | 327.25 | 54.18 | 2.85 | -4.43 | 3 | Yes | High | 40,51 |
| ENDIP | 10.35 ^[b] | 7.71 ^[b] | 2.64 | 1:1 | n.d | 242.32 | 49.84 | 1.27 | -2.79 | 2 | Yes | High | 53 |
| Salan | 9.48 ^[b] | 5.35 ^[b] | 4.13 | 1:1 | N ₂ O _{2eq} | 272.34 | 64.52 | 2.26 | -4.16 | 4 | Yes | High | 47 |
| Salan-1 | 8.97 ^[b] | 5.33 ^[b] | 3.64 | 1:1 | N ₂ O _{2eq} | 656.68 | 245.7 | -1.85 | -1.72 | 10 | No | Low | 62 |
| Salan-2 | 9.83 ^[b] | 5.97 ^[b] | 3.86 | 1:1 | N ₂ O _{2eq} OH ₂ _{ap} | 458.51 | 195.82 | -2.59 | -0.86 | 2 | No | Low | 58,63 |
| Salpyran | 10.65 | 6.69 | 4.60 | 1:1 | N ₃ Cl _{eq} or N _{3eq} Cl _{ap} | 257.33 | 57.18 | 1.73 | -3.47 | 3 | Yes | High | This work |

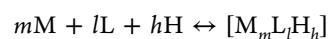
*Constants are for the form Aβ1-x. ^apM = -log[M]_{free}; [M] = [L] = 10 μM, pH = 7.4. ^bCalculated from conditional affinity value. ^cCalculated from apparent affinity value at pH = 7.4. ^dCu/Zn selectivity calculated by pCu - pZn. ^eCoordination environment in solid state; equatorial (eq) and apical (ap) sites. ^fCalculated using the SwissADME free to use webtool; both log P and log S and the consensus values.⁷²

antioxidant properties.⁵⁴ Storr et al. designed multifunctional carbohydrate ligands based around an N-methylated salan core (Salan-1, Figure 2).⁵⁵ The pendant glucose arm facilitates access to the brain and passes through the BBB via glucose transporters. Both ligands were found to have significant antioxidant properties *in vitro*. The O-glycosylation of the Salan ligand was also investigated as a prochelator strategy, where the glucose moiety effectively masks the coordination pocket until hydrolysis occurs *in vivo*.^{56,57} It was confirmed that the enzyme *Agrobacterium* sp. β-glucosidase could effectively cleave the C-O bond of the glucose moiety releasing the N-methylated Salan scaffold as the active chelator at the site. Other attempts to improve the pharmacological profile of the core Salan scaffold have involved the sulfonation of the phenolic groups (Salan-2), which significantly improves solubility (Table 1).⁵⁸ However, it is expected that the presence of an ionizable sulfonate group will result in poor BBB permeability, making it unsuitable for AD treatments. Having all these in mind and building on our recent work in nonsymmetric salan ligands,⁵⁹ we envisaged that the combination of the Salan and Endip moieties should yield a nonsymmetric ligand, Salpyran (Figure 2). By breaking the C₂ symmetry, a new 3N,O coordination environment is formed that may partially fulfill the coordination environment of the Cu(II) center. Salpyran offers the same number of heteroatoms as TDMQ-20. Pearson's acid-base principle predicts that the addition of the pyridine will increase the Cu(II) affinity and selectivity versus the Salan scaffold; this is observed in the trend of pCu values observed for more nitrogen-rich coordination pockets (Table 1). Also, compared to the Salan (cLogP = 2.26, Table 1) scaffold replacement of a phenol with a pyridine entity improves the aqueous solubility by reducing the lipophilicity of the scaffold (cLogP = 1.73, Table 1). However, the phenolic moiety provides the scaffold with radical scavenging capabilities to act as an antioxidant

during AD treatments.⁵⁴ Our approach introduces an entirely different scaffold for use in AD treatment, contrasting the more classical approach of modifying known metal coordinating scaffolds.^{54,56-58,60-63}

Thermodynamic and Physicochemical Properties Compared to Other Cu Chelators.

The selectivity of the ligand for Cu(II) over other metal ions is a critical factor in designing Cu(II) targeting SMMC. The chelator in question should have high selectivity toward copper to minimize competition with other essential metal ions and interactions with other metalloproteins. The stability constant (log β) of the metal complex (ML) is used to assess the affinity of a ligand for a specific metal (eq 1). Therefore, in designing AD therapeutics, it is beneficial to compare the stability constants for Cu(II) and Zn(II) due to the high concentration of Zn(II) in AD brains.^{64,65} The variability in the method and conditions used to measure the metal/ligand affinities has led to the use of the pM (eq 2) value when comparing and assessing the chelation capability of copper targeting SMMCs. The pM value is calculated at physiological pH and micromolar metal and ligand concentrations. Consequently, this offers added benefit by comparing chelators regardless of denticity or metal/ligand stoichiometry.

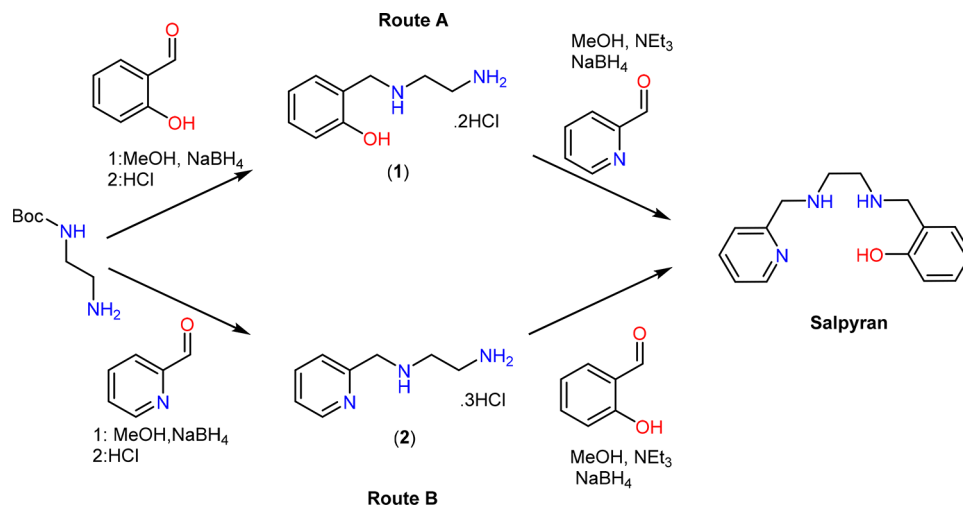


$$\log \beta_{MLH} = \log \left(\frac{[M_mL_lH_h]}{[M]_m [L]_l [H]_h} \right) \quad (1)$$

$$pM = -\log[M]_{\text{free}} \quad (2)$$

Synthesis of Salpyran. Salpyran can be synthesized via a stepwise protecting group strategy in which consecutive reductive aminations using salicylaldehyde and 2-formylpyridine take place across an ethylenediamine backbone (Scheme 1, Figures S1-S10). First, the reductive amination of either

Scheme 1. Two Alternate Synthetic Routes Towards Salpyran Starting from *N*-Boc-ethylenediamine and Using Either (A) Salicylaldehyde or (B) 2-Formylpyridine



aldehyde with *N*-Boc-ethylenediamine and subsequent deprotection give the amine precursors (1) and (2) (Scheme 1). A second reductive amination, this time in the presence of stoichiometric base (NEt_3), yields **Salpyran**. It is possible to modify **Salpyran** via variation in the aromatic substitution of either aldehyde or by replacement of the diamine linker unit. Functionalization is also possible at either of the amine's groups, making **Salpyran** a highly tunable scaffold compared to similar symmetric structures. For this three-step synthesis, the total yield of **Salpyran** via route A is 49% and significantly drops to 19% for route B. The fact that there are two simple synthetic routes demonstrates the synthetic accessibility toward **Salpyran**, which offers flexibility in analogue design in further medicinal chemistry pursuits. In the development of drugs targeting neurodegenerative disorders, there has been a trend in the design of multifunctional drugs that contain structural moieties aiming to target multiple pathological features at once or the addition of bioisosteres or isosteres to modify the pharmacokinetic properties.⁶⁶ This has led to an interest in multifunctional drugs containing a metal-binding unit;^{67–69} therefore, the high synthetic accessibility and tunability of **Salpyran** may offer future opportunities for use in multifunctional drugs.

Complexation Behavior with Cu(II) and Zn(II). The protonation constants (Table S1) of **Salpyran** were determined by pH-metric titrations. Using these data, the stability constants of the Cu(II) and Zn(II) complexes were calculated (Table 2). At low pH (<4) values, the dicationic $[\text{CuLH}]^{2+}$ is the dominant species. At the same time, the phenolic hydroxyl group remains protonated and uncoordinated. Across the physiological pH values (7.4), the

monocationic $[\text{CuL}]^+$ is the dominant species. In contrast, at high pH values (>11), a further deprotonation process occurs, forming a neutral $[\text{CuLH}_{-1}]$ species likely via the deprotonation of a coordinated water molecule (Figure 3A,B). The aqueous solution behavior is alike for Zn(II); however, no protonated complex is formed. At pH 5, 50% of Zn(II) is found unbound (Figure 3C). In all, the stability of the formed Zn(II) species is lower than that of the corresponding Cu(II) species, demonstrating the Cu(II) selectivity of **Salpyran** (Table 1). The species distribution plots of the Cu(II) complexes formed in equimolar metal to ligand solutions are shown in Figure 3. Further solution studies with Cu(II) were performed in a mixture of DMSO:H₂O (70:30), as it is a common practice for biological studies. Notably, the ligand behavior changes drastically, corroborated by UV–vis studies (Figure 3D,E), showcasing the formation of other species and indicating that speciation is highly dependent on the solvent system (Table S2). In the less polar DMSO-containing solvent mixture, the positively charged $[\text{CuL}]^+$ species is dominant in both systems in the physiological pH range (Figure 3) but is present in a narrower pH range, and the formation of the neutral $[\text{CuLH}_{-1}]$ species is favorable. Based on this evidence, we considered that solution studies in DMSO solution would add no value to our conclusion.

The complex formation of **Salpyran** with Cu(II) and Zn(II) ions was studied at 1:2 and 1:1 ligand to metal ion ratios in the pH range 3–11 (Figure S11). Comparison of the UV–vis spectra of the Cu(II)-**Salpyran** system at 1:2 and 1:1 metal to ligand ratios (Figure S12) shows that similar spectra are obtained. These studies indicate that irrespectively of the metal to ligand ratio, only the 1:1 complex forms at pH values ranging from 3 to 11. Therefore, we assume that during *in vivo* studies, the 1:1 species is dominant, reducing the possibility of interactions with endogenous metalloproteins.

The thermodynamic properties and drug-likeness of **Salpyran** and other chelators discussed in this work are summarized in Table 1. The affinity of the ligands for Cu(II) and Zn(II) is measured using pCu and pZn values calculated from the reported conditional ($\log \beta_{\text{con}}$) or apparent ($\log \beta_{\text{app}}$) stability constants using $[\text{M}] = [\text{L}] = 10 \mu\text{M}$, p.H = 7.4. This was achieved using the Hyperquad simulation and speciation (HySS) software.⁷¹ Copper/zinc selectivity is given as pCu/276

Table 2. Stability Constants ($\log \beta$) for **Salpyran complexes with Cu(II) and Zn(II) in Aqueous Solution Calculated Using the SUPERQUAD software (ref 70)***

| $\log \beta$ | Cu(II) | Zn(II) |
|-------------------|-----------|-----------|
| MLH | 23.93 (8) | — |
| ML | 20.10 (8) | 11.98 (5) |
| MLH ₋₁ | 8.94 (10) | 2.38 (13) |

* $I = 0.2 \text{ mol} \times \text{dm}^{-3} \text{ KCl}$, $T = 298 \text{ K}$, standard deviations are in parentheses.

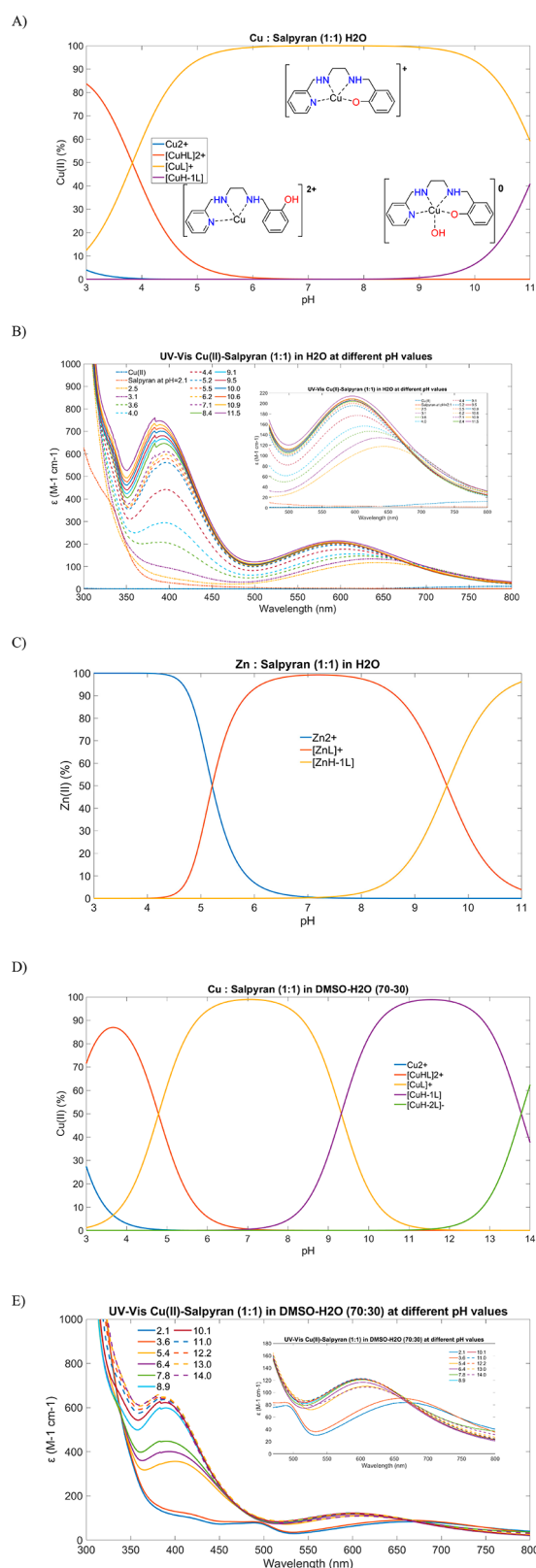


Figure 3. (A, B) Species distribution and UV-vis data of the Cu(II)-Salpyran complexes formed in the equimolar solutions as a function of pH in H₂O. (C) Species distribution of the Zn(II)-Salpyran complexes formed in the equimolar solutions as a function of pH. (D, E) Species distribution and UV-vis data of the Cu(II)-Salpyran complexes formed in the equimolar solutions as a function of pH in mixture DMSO:H₂O (70:30).

pZn; the larger the value, the greater selectivity toward Cu(II) over Zn(II). Also included in Table 1 is the stoichiometry and coordination environment of the copper complexes according to the reported solid-state structures. The drug-likeness of the ligands has been predicted using the SwissADME web tool and the calculated physicochemical properties and predicted BBB permeation and gastrointestinal absorption are also given.⁷² Ideally, any SMMC would follow the 'Lipinski rule of 5',⁷³ and have a topological polar surface not exceeding 140 Å² (Veber rule).⁷⁴ In all, the complexation behavior of Salpyran supports its potential use as a Cu(II) targeting SMMC. It has an exceptional affinity for Cu(II) (pCu = 10.65) and good selectivity for Cu(II) over Zn(II) (Cu/Zn = 4.60) (Table 1). Salpyran acts as a tridentate or tetradentate, dependent on the pH and only forms the 1:1 complex with Cu(II). (The characteristic bands of the Cu(II) complexes are summarized in Table S3.) Salpyran has a higher affinity and selectivity for copper when compared to its C₂ symmetric analogues, ENDIP and Salan and comparable affinity but with lower selectivity when compared to TMDQ-20 (Table 1).

From Table 1, it is evident that Salpyran offers both high affinity and selectivity for Cu(II) (pCu = 10.65, Cu/Zn = 4.6). Compared to both "parent" ligands, EDNIP and Salan, Salpyran outperforms, and its values are close to the state of the art TMDQ-20 (pCu = 10.75, Cu/Zn = 5.06). Salpyran has good solubility, and its calculated log P value suggests that good BBB permeation could be expected, although the number of hydrogen bond donors (HBD = 3) may be deleterious to BBB influx and may need to be factored into future drug design (e.g., masked HBDs, rigidification).^{80,81}

Salpyran Copper Crystal Structure. To better understand the complexation behavior of Salpyran with Cu(II), we carried out several complexation reactions in protic or aprotic solvents. The reflux of an equimolar solution of Salpyran, CuCl₂, and NEt₃ for 1 h in methanol yielded a viscous, green oil, which upon dissolving in DMF, followed by vapor diffusion of diethyl ether over 1 week, yielded blue crystals suitable for single X-ray diffraction in low yield (13%, Tables S4 and S5). The solid-state structure is shown in Figure 4. Upon complexation with CuCl₂, Salpyran yields an asymmetric Cu(II)-dimer consisting of two different (CuCl₂HL) units, and Cl₂ serves as a bridge of these two entities. The coordination geometry of the two Cu centers varies; Cu1 adopts a 3N,2Cl coordination environment (square pyramidal), while Cu2 adopts a 3N,3Cl environment (distorted octahedron) (Figure 4); notably, both phenol moieties remain protonated. This observation is in line with the potentiometric studies, which suggest that at low pH values (pH < 4), the [CuHL]₂²⁺ species is dominant. The crystal structure confirms that the ligands exhibit two five-membered chelated rings via coordination of the three nitrogen donor atoms (NH, NH, N_{py}), which may account for the high stability of [CuHL]₂²⁺ species (Table 1). Moreover, a close inspection of bond lengths and angles (Table S3) reveals three different Cu-Cl bond types: Cl2 and Cl3 strongly bind to Cu1 and Cu2, respectively, [2.2780(14) Å and 2.2649(15) Å], the Cu1-Cl1 [2.6466(15) Å] and Cu2-Cl4 [2.7294(15) Å] are weakened bonds, while the value of the Cu2-Cl2 bond is 3.0454(15) Å, which is indicative of a secondary, very weak interaction.⁸²

Further attempts to isolate crystals of the complex with the deprotonated ligand were unsuccessful. HRMS of the isolated crystals and viscous green oil is provided in the Supporting Information (Figures S13 and S14) and is in line with the

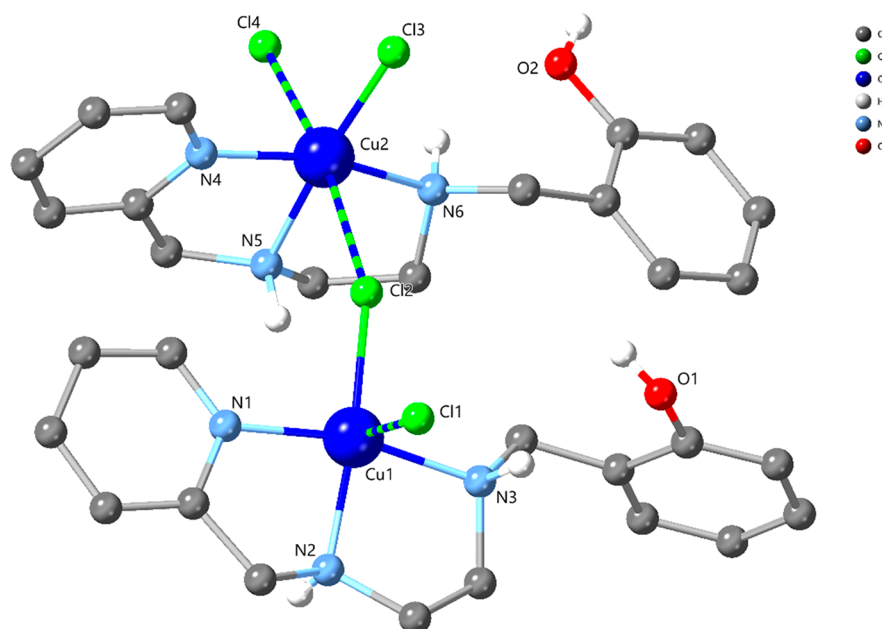


Figure 4. Solid-state structure of protonated Salpyran–copper complex.

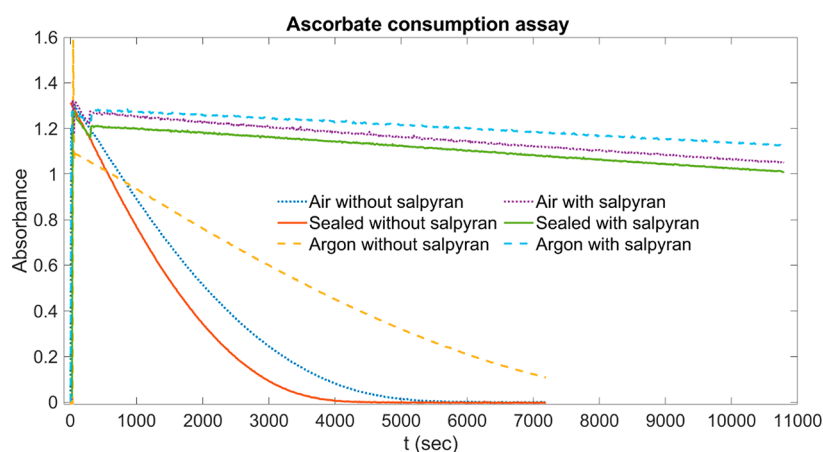


Figure 5. Kinetics of ascorbate consumption with(out) Salpyran in different conditions (open air, Ar, and sealed cuvette). The reactants Salpyran (if any)/CuCl₂/ascorbate (12 μM/10 μM/100 μM) ratio.

340 [CuL]⁺ and [CuHL]²⁺ structures, respectively. In all, taking
 341 into account that (a) differentiation in Cu–Cl bonding is due
 342 to the weakly binding character of the Cl anion, (b) solution
 343 studies were carried out using CuCl₂ stock solutions, (c) UV–
 344 vis studies suggest the existence of a Cu₂3N (low pH value)
 345 and Cu₂3N₂O (physiological pH values) chromophores, and
 346 (d) ESI-MS studies corroborate the existence of monomeric,
 347 not dimeric species, in methanolic or aqueous solution, we can
 348 correlate the solid and solution phases and confirm the
 349 dominance of the [CuL]⁺ species at physiological pH values.

350 **Antioxidant Properties.** Redox-active Cu(II) is known to
 351 induce ROS formation and oxidative stress accumulation.⁸³
 352 Therefore, potential therapeutic SMMCs must be capable of
 353 effectively inhibiting Cu(II)-induced ROS formation. As a
 354 starting point, we adopted a recently reported protocol⁸³ and
 355 investigated the ability of Salpyran to arrest the ROS
 356 production by monitoring ascorbate consumption under
 357 three different conditions (open air, Ar, and sealed cuvette).
 358 The ascorbate consumption is plotted as a function of time in
 359 seconds (Figure 5 and Figures S15–S20). The ascorbate

consumption without Salpyran was followed for 2 h, while in
 the presence of Salpyran, the samples were monitored for 3 h.
 Samples were prepared in situ from stock solutions in 100 mM
 HEPES buffer at pH 7.1, and the pH was adjusted with 0.2 M
 HCl. The components were added in the following order:
 HEPES, HCl, water, ascorbate, CuCl₂, and Salpyran (if any).
 The assay was carried out under anaerobic and aerobic
 conditions. In the anaerobic studies, the ascorbate con-
 sumption was not completed even after 2 h, while under
 aerobic conditions, the ascorbate is fully consumed in 1.5 h.
 The calculated rate constants (from 5000 to 10,000 s, Table 3)
 for the samples containing Salpyran are under argon, 1.07 ×
 10^{−9} Ms^{−1} (=1.07 nMs^{−1}), in open air, 1.37 × 10^{−9} Ms^{−1} (1.37
 nMs^{−1}), and in a sealed cuvette, 1.36 × 10^{−9} Ms^{−1} (=1.36
 nMs^{−1}). The rate constants were calculated by dividing the
 slope by the extinction coefficient of ascorbate, ε = 14,500 M^{−1}
 cm^{−1}. Any difference in rates with the reported protocol⁸³ may
 be attributed to the stirring rate (300 rpm over 800 rpm) and
 ligand framework. These studies clearly show Salpyran slows

Table 3. Calculated Rate Constants* for Kinetics of Ascorbate Consumption in Different Conditions with Ratio Salpyran/CuCl₂/Ascorbate (12 μM/10 μM/100 μM)

| Condition | Without Salpyran | With Salpyran |
|-----------|------------------|---------------|
| Air | Not calculated | 1.37 |
| Sealed | Not calculated | 1.36 |
| Argon | Not calculated | 1.07 |

*In nMs⁻¹.

the ascorbate consumption, thus demonstrating its capability to prevent ROS production.

Also, we investigated Salpyran's oxidation ability in the presence of H₂O₂ (Figure 6 and Figures S21 and S22). The reaction mixtures containing 1.0 mM Salpyran at metal to ligand molar ratio 1:1 were incubated at 25 °C for different time periods in the presence of H₂O₂ at ligand to H₂O₂ molar ratio 1:4. The pH was adjusted to 7.4. The reaction was initiated by the addition of a freshly prepared 1% H₂O₂ solution. The reaction was stopped by the addition of Na₂EDTA at ligand to Na₂EDTA ratio 1:5. The reaction process was monitored by analytical RP-HPLC using a Jasco instrument, equipped with a Jasco MD-2010 plus a multi-

wavelength detector. From these data, it is evident that oxidation does not occur in the sample containing equivalent amount of Cu(II) and Salpyran even after 2 days (Figure S21, upper). While in the sample containing 4-fold excess 1% H₂O₂, some oxidation occurs in the first 4 h (Figure S21, lower).

Then, we assessed the ability of Salpyran in preventing Cu(II)-catalyzed oxidation in two different protein fragment assays at physiological pH values. It has previously been shown that a fragment of the human prion protein (HuPrP(103–112), dMKHM) (Figure S23) undergoes oxidation in the presence of radicals formed from the Cu(II)/H₂O₂ system.⁸⁴ The oxidation occurs only at the methionine residues, yielding three main products: two singly oxidized products (dMKHM + O, orange) and a doubly oxidized product (dMKHM + 2O, yellow). Both methionine residues at position 7 (Met109) or/and at position 10 (Met112) can be oxidized. However, only methionine sulfoxides are produced and not the corresponding sulfones. The oxidation was initiated by adding H₂O₂ to an equimolar Cu(II)-dMKHM-Salpyran solution, and the reaction was monitored by HPLC for 1 day (Figure 7). After 1 h, almost 60% of HuPrP(103–112) remains intact, and no oxidation occurs in any methionine group, three times higher than the blank experiment. In contrast, after 2 h, the

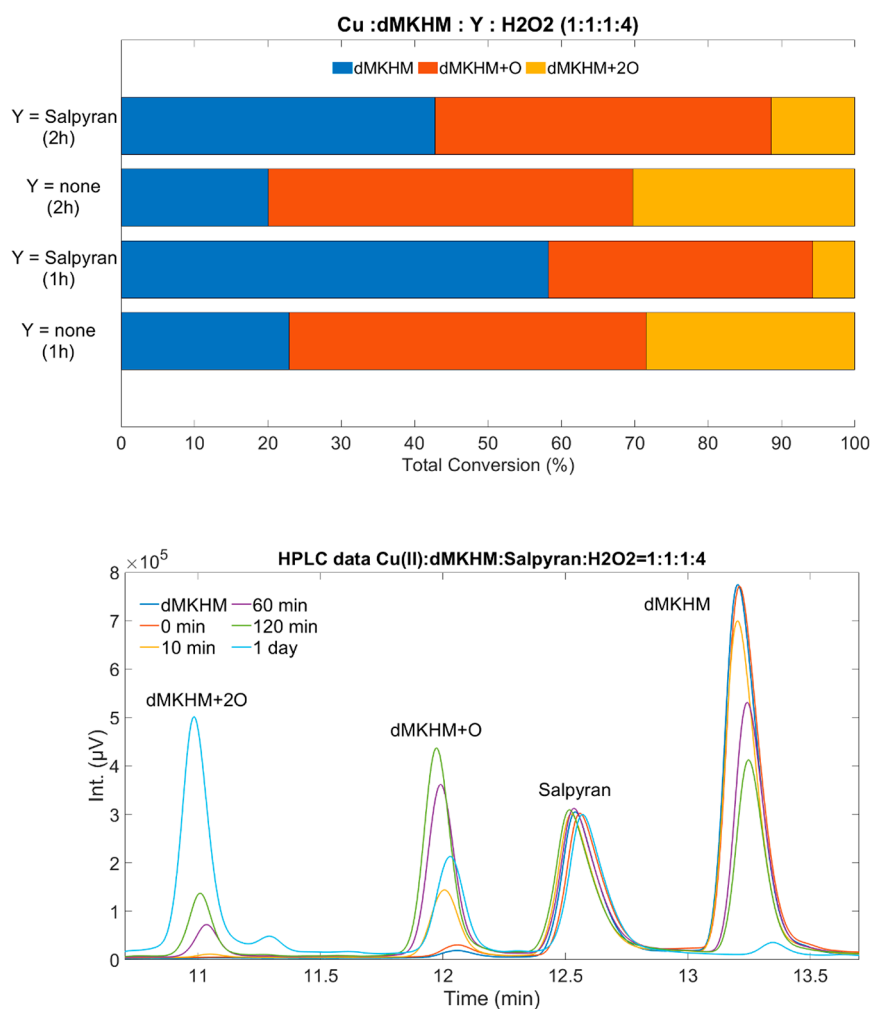


Figure 6. (upper) Ratio of the Cu(II)/H₂O₂ oxidized prion protein fragment, HuPr(103–112) (dMKHM), formed products with and without Salpyran. (lower) An HPLC chromatograph of the oxidation process 0 min, 10 min, 60 min, 120 min, and 1 day. Teknokroma Europa Protein C18 (250 × 4.6 mm, 300 Å, 5 μm) column at a flow rate of 1 mL·min⁻¹, monitoring the absorbance at 222 nm. Mobile phases were water (A) and acetonitrile (B) containing 0.1% TFA.

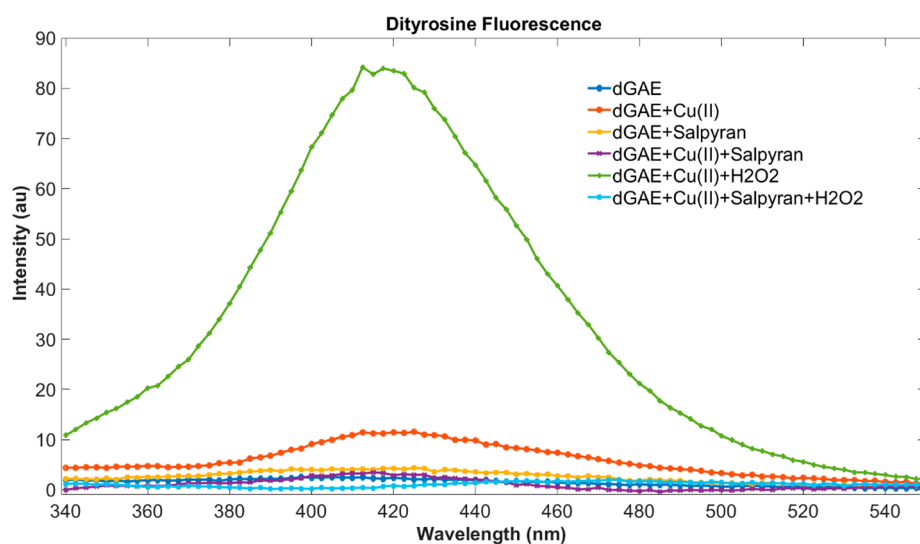


Figure 7. Fluorescence monitoring of the formation of dityrosine bridges from Cu(II)/H₂O₂ oxidation of the tau dGAE fragment. Reactions were prepared using μ M dGAE mixed with Cu(II) at a 1:10 ratio or in combination with 2.5 mM H₂O₂ to induce oxidation and dityrosine cross-linking. A separate dGAE reaction was prepared with Salpyran at a 1:10 ratio or Salpyran in combination with Cu(II) at a 1:1 ratio alone and in combination with 2.5 mM H₂O₂. The reactions were quenched after 1 h with the addition of 2 mM EDTA.

percentage of dMKHM is still high (40%, doubled compared to that of the blank), while unreacted dMKHM parts are still evident after 1 day (HPLC, Figure 6). These data demonstrate Salpyran's efficiency in hindering the oxidation of the peptide, possibly by protecting the Cu(II) ions and inhibiting the ROS formation from the binary Cu(II)/H₂O₂ system. The lack of total inhibition of peptide oxidation was not observed, potentially due to an excess of peroxide used in the experiment. These results demonstrate the potential of Salpyran in targeting Cu(II) dyshomeostasis and reducing the oxidative stress associated with neuronal death.

One known product of oxidation induced by Cu(II) is dityrosine cross-links on proteins, such as A β .⁸⁵ Dityrosine (DiY) formation, whereby closely spaced tyrosines covalently cross-link by ortho–ortho coupling at C3 of their benzene rings, has been used as a marker of oxidative stress, and DiY has been shown to form under Cu(I/II)/H₂O₂ oxidative conditions for A β and tau *in vitro*^{86–89} and within AD amyloid plaques *in vivo*.⁸⁷ In the presence of H₂O₂, Cu(II) induces dityrosine cross-linking more efficiently, serving as an excellent marker of oxidation.⁸⁹ Also, Cu(II) is known to bind tau and induce tau oxidation, dimerization, and aggregation.^{90,91} Recently, it was demonstrated that Cu(II) alone or in the presence of H₂O₂ induces oxidation and dityrosine cross-linking of a tau297–391 fragment which contains one tyrosine at position 310.^{89,92} To further demonstrate the antioxidant ability of Salpyran, we performed a series of reactions using tau297–391 and Cu(II) (1:10 ratio) in combination with H₂O₂ to induce oxidation and dityrosine formation, which were quenched after 1 h with the addition of EDTA. The appearance of the dityrosine species was observed by monitoring the intensity of the peak at 410 nm (Figure 7). Unlike the reactions with just Cu(II) or more so in combination with H₂O₂, which showed robust induction of dityrosine to approximately 1% and 7% dityrosine levels (Figure S24), similar reactions mixed with Salpyran showed no dityrosine cross-linking alongside the controls (below 0.5%) (Figure 7). This suggests that Salpyran effectively prevents dityrosine formation and thus oxidation of dGAE via binding

to Cu(II). Combined with the aforementioned antioxidant studies, these results indicate that Salpyran can reduce ROS production in both Cu(II)/H₂O₂ and Cu(II)/O₂/reductant systems.

CONCLUSION

We rationally designed and synthesized a highly modifiable copper chelating scaffold, Salpyran. This tetradentate ligand offers a 3N,O coordination environment and possesses good drug-likeness. Salpyran exhibits an extremely high affinity for Cu and excellent Cu(II) selectivity over Zn(II), comparable to the state of the art components. Solid and solution studies corroborate variation in coordination behavior at different pH values, but confirm the existence of only one dominant species at physiological pH values in aqueous solutions. Under physiological pH values and unaerobic conditions, the [Cu(II)(3N,1O)]⁺ complex remains intact for at least 2 days, while in the presence of H₂O₂, an oxidation procedure occurs. Further studies showcase that Salpyran slows the ascorbate consumption, thus preventing ROS production. Finally, two different protein fragment assays that investigate antioxidant properties revealed Salpyran's excellent efficacy to prevent the formation of ROS from Cu(II)/H₂O₂. Due to its drug-likeness, desirable coordination behavior, antioxidant properties, and tunability, Salpyran is an alternative scaffold to 8-hydroxy/aminoquinolines for further pharmaceutical development of Cu(II) targeting drugs in neurodegenerative disorders such as AD.

ASSOCIATED CONTENT

Supporting Information

The Supporting Information is available free of charge at <https://pubs.acs.org/doi/10.1021/acs.inorgchem.1c01912>.

Copies of ¹H, ¹³C NMR, HRMS, and LCMS data for the ligand (PDF)

Accession Codes

CCDC 2090343 contains the supplementary crystallographic data for this paper. These data can be obtained free of charge

490 via www.ccdc.cam.ac.uk/data_request/cif, or by emailing
491 data_request@ccdc.cam.ac.uk, or by contacting The Cam-
492 bridge Crystallographic Data Centre, 12 Union Road,
493 Cambridge CB2 1EZ, UK; fax: +44 1223 336033.

494 ■ AUTHOR INFORMATION

495 Corresponding Authors

496 **George E. Kostakis** – Department of Chemistry, School of Life
497 Sciences, University of Sussex, Brighton BN1 9QJ, United
498 Kingdom; orcid.org/0000-0002-4316-4369;
499 Email: G.Kostakis@sussex.ac.uk

500 **John Spencer** – Department of Chemistry, School of Life
501 Sciences, University of Sussex, Brighton BN1 9QJ, United
502 Kingdom; orcid.org/0000-0001-5231-8836;
503 Email: j.spencer@sussex.ac.uk

504 **Csilla Kállay** – Department of Inorganic and Analytical
505 Chemistry, University of Debrecen, H-4032 Debrecen,
506 Hungary; Email: kallay.csilla@science.unideb.hu

507 Authors

508 **Jack Devonport** – Department of Chemistry, School of Life
509 Sciences, University of Sussex, Brighton BN1 9QJ, United
510 Kingdom

511 **Nikolett Bodnár** – Department of Inorganic and Analytical
512 Chemistry, University of Debrecen, H-4032 Debrecen,
513 Hungary

514 **Andrew McGown** – Department of Chemistry, School of Life
515 Sciences, University of Sussex, Brighton BN1 9QJ, United
516 Kingdom

517 **Mahmoud Bukar Maina** – Sussex Neuroscience, School of Life
518 Sciences, University of Sussex, Brighton BN1 9QJ, United
519 Kingdom; College of Medical Sciences, Yobe State University,
520 PMB 1144 Damaturu, Yobe State, Nigeria

521 **Louise C. Serpell** – Sussex Neuroscience, School of Life
522 Sciences, University of Sussex, Brighton BN1 9QJ, United
523 Kingdom; orcid.org/0000-0001-9335-7751

524 Complete contact information is available at:

525 <https://pubs.acs.org/10.1021/acs.inorgchem.1c01912>

526 Author Contributions

527 All authors contributed to writing the manuscript and
528 approved its final version. J.D. devised the project with critical
529 input and comments from G.E.K, J.S., and C.K. J.D. designed,
530 synthesized, and characterized the ligand and performed and
531 evaluated, with G.E.K., the crystallographic data. C.K. and N.B.
532 performed and evaluated the potentiometry, UV–vis, and
533 human prion fragment studies. L.S. and M.B.M. performed and
534 evaluated the dityrosine studies. A.M. provided valuable
535 feedback and comments.

536 Notes

537 The authors declare no competing financial interest.

538 ■ ACKNOWLEDGMENTS

539 G.E.K. and J.S. received funding from the School of Life
540 Sciences, the University of Sussex (J.D. Ph.D. fellowship). C.K.
541 and N.B. thank the Hungarian Scientific Research Fund
542 (NKFI-115480 and NKFI- 124983) for its financial support.
543 The research was also supported by the János Bolyai Research
544 Scholarship of the Hungarian Academy of Sciences and by the
545 ÚNKP-20-5 New National Excellence Program of the Ministry
546 for Innovation and Technology from the source of the
547 National Research, Development, and Innovation Fund. M.M.

is funded by Alzheimer's Society (AS-PG-16b-010). L.C.S. is
supported by funding from BBSRC (BB/S003657/1). 549

550 ■ REFERENCES

- 551 Toni, M.; Massimino, M. L.; De Mario, A.; Angiulli, E.; Spisni, E. 552 Metal Dyshomeostasis and Their Pathological Role in Prion and 553 Prion-like Diseases: The Basis for a Nutritional Approach. *Front. 554 Neurosci.* **2017**, *11* (JAN), 3. 555
- 556 (2) Sayre, L. M.; Moreira, P. I.; Smith, M. A.; Perry, G. Metal Ions 557 and Oxidative Protein Modification in Neurological Disease. *Ann. Ist. 558 Super. Sanita* **2005**, *41* (2), 143–164. 559
- 560 (3) Bonda, D. J.; Lee, H. G.; Blair, J. A.; Zhu, X.; Perry, G.; Smith, 561 M. A. Role of Metal Dyshomeostasis in Alzheimer's Disease. *562 Metallomics* **2011**, *3* (3), 267–270. 563
- 564 (4) Bolognin, S.; Messori, L.; Zatta, P. Metal Ion Physiopathology in 565 Neurodegenerative Disorders. *NeuroMol. Med.* **2009**, *11* (4), 223– 566 238. 567
- 568 (5) Zhou, C.; Huang, Y.; Przedborski, S. Oxidative Stress in 569 Parkinson's Disease: A Mechanism of Pathogenic and Therapeutic 570 Significance. *Ann. N. Y. Acad. Sci.* **2008**, *1147*, 93–104. 571
- 572 (6) Ayton, S.; Lei, P.; Bush, A. I. Metallostasis in Alzheimer's 573 Disease. *Free Radical Biol. Med.* **2013**, *62*, 76–89. 574
- 575 (7) Barnham, K. J.; Masters, C. L.; Bush, A. I. Neurodegenerative 576 Diseases and Oxidative Stress. *Nat. Rev. Drug Discovery* **2004**, *3* (3), 577 205–214. 578
- 579 (8) Bush, A. I. Metals and Neuroscience. *Curr. Opin. Chem. Biol.* 580 **2000**, *4* (2), 184–191. 581
- 582 (9) Greenough, M. A.; Camakaris, J.; Bush, A. I. Metal Dyshomeo- 583 stasis and Oxidative Stress in Alzheimer's Disease. *Neurochem. Int.* 584 **2013**, *62* (5), 540–555. 585
- 586 (10) Lane, C. A.; Hardy, J.; Schott, J. M. Alzheimer's Disease. *Eur. J.* 587 *Neurol.* **2018**, *25* (1), 59–70. 588
- 589 (11) *World Alzheimer Report 2018*; Alzheimer's Disease Interna- 590 tional: London, 2018. 591
- 592 (12) Mayeux, R.; Stern, Y. Epidemiology of Alzheimer Disease. *Cold 593 Spring Harbor Perspect. Med.* **2012**, *2* (8), a006239. 594
- 595 (13) Ferri, C. P.; Prince, M.; Brayne, C.; Brodaty, H.; Fratiglioni, L.; 596 Ganguli, M.; Hall, K.; Hasegawa, K.; Hendrie, H.; Huang, Y.; Jorm, 597 A.; Mathers, C.; Menezes, P. R.; Rimmer, E.; Sczufca, M. Global 598 Prevalence of Dementia: A Delphi Consensus Study. *Lancet* **2005**, 599 *366* (9503), 2112–2117. 600
- 601 (14) Fratiglioni, L. Epidemiology of Alzheimer's Disease. Issues of 602 Etiology and Validity. *Acta Neurol. Scand. Suppl.* **1993**, *145*, 1–70. 603
- 604 (15) Bush, A. I.; Pettingell, W. H.; Multhaup, G.; Paradis, M. D.; 605 Vonsattel, J. P.; Gusella, J. F.; Beyreuther, K.; Masters, C. L.; Tanzi, R. 606 E. Rapid Induction of Alzheimer A β Amyloid Formation by Zinc. 607 *Science* **1994**, *265* (5177), 1464–1467. 608
- 609 (16) Huang, X.; Atwood, C. S.; Hartshorn, M. A.; Multhaup, G.; 610 Goldstein, L. E.; Scarpa, R. C.; Cuajungco, M. P.; Gray, D. N.; Lim, J.; 611 Moir, R. D.; Tanzi, R. E.; Bush, A. I. The A β Peptide of Alzheimer's 612 Disease Directly Produces Hydrogen Peroxide through Metal Ion 613 Reduction. *Biochemistry* **1999**, *38* (24), 7609–7616. 614
- 615 (17) Atwood, C. S.; Huang, X.; Moir, R. D.; Tanzi, R. E.; Bush, A. I. 616 Role of Free Radicals and Metal Ions in the Pathogenesis of 617 Alzheimer's Disease. *Met. Ions Biol. Syst.* **1999**, *36*, 309–364. 618
- 619 (18) Bush, A. I. The Metallobiology of Alzheimer's Disease. *Trends* 620 *Neurosci.* **2003**, *26* (4), 207–214. 621
- 622 (19) Maynard, C. J.; Bush, A. I.; Masters, C. L.; Cappai, R.; Li, Q.-X. 623 Metals and Amyloid- β in Alzheimer's Disease. *Int. J. Exp. Pathol.* 624 **2005**, *86* (3), 147–159. 625
- 626 (20) Schrag, M.; Mueller, C.; Oyoyo, U.; Smith, M. A.; Kirsch, W. 627 M. Iron, Zinc and Copper in the Alzheimer's Disease Brain: A 628 Quantitative Meta-Analysis. Some Insight on the Influence of Citation 629 Bias on Scientific Opinion. *Prog. Neurobiol.* **2011**, *94* (3), 296–306. 630
- 631 (21) Cilliers, K. Trace Element Alterations in Alzheimer's Disease: A 632 Review. *Clin. Anat.* **2021**, *34* (5), 766–773. 633
- 634 (22) Kabir, M. T.; Uddin, M. S.; Zaman, S.; Begum, Y.; Ashraf, G. 635 M.; Bin-Jumah, M. N.; Bungau, S. G.; Mousa, S. A.; Abdel-Daim, M. 636

- 615 M. Molecular Mechanisms of Metal Toxicity in the Pathogenesis of
616 Alzheimer's Disease. *Mol. Neurobiol.* **2021**, *58* (1), 1–20.
- 617 (23) Cummings, J.; Lee, G.; Ritter, A.; Sabbagh, M.; Zhong, K.
618 Alzheimer's Disease Drug Development Pipeline: 2019. *Alzheimer's*
619 *Dementia Transl. Res. Clin. Interv.* **2019**, *5*, 272–293.
- 620 (24) Cummings, J.; Lee, G.; Ritter, A.; Sabbagh, M.; Zhong, K.
621 Alzheimer's Disease Drug Development Pipeline: 2020. *Alzheimer's*
622 *Dementia Transl. Res. Clin. Interv.* **2020**, *6* (1), No. e12050.
- 623 (25) Cummings, J.; Aisen, P. S.; Dubois, B.; Frölich, L.; Jack, C. R.;
624 Jones, R. W.; Morris, J. C.; Raskin, J.; Dowsett, S. A.; Scheltens, P.
625 Drug Development in Alzheimer's Disease: The Path to 2025.
626 *Alzheimer's Res. Ther.* **2016**, *8* (1), 1–12.
- 627 (26) Cummings, J. L.; Morstorf, T.; Zhong, K. Alzheimer's Disease
628 Drug-Development Pipeline: Few Candidates, Frequent Failures.
629 *Alzheimer's Res. Ther.* **2014**, *6* (4), 37.
- 630 (27) Viles, J. H. Metal Ions and Amyloid Fiber Formation in
631 Neurodegenerative Diseases. Copper, Zinc and Iron in Alzheimer's,
632 Parkinson's and Prion Diseases. *Coord. Chem. Rev.* **2012**, *256* (19–
633 20), 2271–2284.
- 634 (28) Hureau, C. Coordination of Redox Active Metal Ions to the
635 Amyloid Precursor Protein and to Amyloid- β Peptides Involved in
636 Alzheimer Disease. Part 1: An Overview. *Coord. Chem. Rev.* **2012**, *256*
637 (19–20), 2164–2174.
- 638 (29) Barnham, K. J.; Bush, A. I. Biological Metals and Metal-
639 Targeting Compounds in Major Neurodegenerative Diseases. *Chem.*
640 *Soc. Rev.* **2014**, *43* (19), 6727–6749.
- 641 (30) Perry, G.; Cash, A. D.; Smith, M. A. Alzheimer Disease and
642 Oxidative Stress. *J. Biomed. Biotechnol.* **2002**, *2* (3), 120–123.
- 643 (31) Cheignon, C.; Tomas, M.; Bonnefont-Rousselot, D.; Faller, P.;
644 Hureau, C.; Collin, F. Oxidative Stress and the Amyloid Beta Peptide
645 in Alzheimer's Disease. *Redox Biol.* **2018**, *14*, 450–464.
- 646 (32) Pohanka, M. Alzheimer's Disease and Oxidative Stress: A
647 Review. *Curr. Med. Chem.* **2013**, *21* (3), 356–364.
- 648 (33) Cuajungco, M. P.; Faget, K. Y.; Huang, X.; Tanzi, R. E.; Bush,
649 A. I. Metal Chelation as a Potential Therapy for Alzheimer's Disease.
650 *Ann. N. Y. Acad. Sci.* **2000**, *920* (1), 292–304.
- 651 (34) Bush, A. I.; Tanzi, R. E. Therapeutics for Alzheimer's Disease
652 Based on the Metal Hypothesis. *Neurotherapeutics* **2008**, *5* (3), 421–
653 432.
- 654 (35) Robert, A.; Liu, Y.; Nguyen, M.; Meunier, B. Regulation of
655 Copper and Iron Homeostasis by Metal Chelators: A Possible
656 Chemotherapy for Alzheimers Disease. *Acc. Chem. Res.* **2015**, *48* (5),
657 1332–1339.
- 658 (36) Adlard, P. A.; Bush, A. I. Metals and Alzheimer's Disease: How
659 Far Have We Come in the Clinic? *J. Alzheimer's Dis.* **2018**, *62*, 1369–
660 1379.
- 661 (37) Singh, Y. P.; Pandey, A.; Vishwakarma, S.; Modi, G. A Review
662 on Iron Chelators as Potential Therapeutic Agents for the Treatment
663 of Alzheimer's and Parkinson's Diseases. *Mol. Diversity* **2019**, *23* (2),
664 509–526.
- 665 (38) Ceccom, J.; Coslédan, F.; Halley, H.; Francès, B.; Lassalle, J.
666 M.; Meunier, B. Copper Chelator Induced Efficient Episodic Memory
667 Recovery in a Non-Transgenic Alzheimer's Mouse Model. *PLoS One*
668 **2012**, *7* (8), e43105.
- 669 (39) Esmieu, C.; Guettas, D.; Conte-Daban, A.; Sabater, L.; Faller,
670 P.; Hureau, C. Copper-Targeting Approaches in Alzheimer's Disease:
671 How to Improve the Fallouts Obtained from in Vitro Studies. *Inorg.*
672 *Chem.* **2019**, *58* (20), 13509–13527.
- 673 (40) Li, Y.; Nguyen, M.; Baudoin, M.; Vendier, L.; Liu, Y.; Robert,
674 A.; Meunier, B. Why Is Tetradentate Coordination Essential for
675 Potential Copper Homeostasis Regulators in Alzheimer's Disease?
676 *Eur. J. Inorg. Chem.* **2019**, *2019* (44), 4712–4718.
- 677 (41) Aaseth, J.; Skaug, M. A.; Cao, Y.; Andersen, O. Chelation in
678 Metal Intoxication-Principles and Paradigms. *J. Trace Elem. Med. Biol.*
679 **2015**, *31*, 260–266.
- 680 (42) Perez, L. R.; Franz, K. J. Minding Metals: Tailoring
681 Multifunctional Chelating Agents for Neurodegenerative Disease.
682 *Dalton Trans.* **2010**, *39* (9), 2177–2187.
- (43) Pardridge, W. M. Alzheimer's Disease Drug Development and
683 the Problem of the Blood-Brain Barrier. *Alzheimer's Dementia* **2009**, *5*
684 (5), 427–432.
- (44) Ritchie, C. W.; Bush, A. I.; Mackinnon, A.; Macfarlane, S.;
685 Mastwyk, M.; MacGregor, L.; Kiers, L.; Cherny, R.; Li, Q. X.;
686 Tammer, A.; Carrington, D.; Mavros, C.; Volitakis, I.; Xilinas, M.;
687 Ames, D.; Davis, S.; Beyreuther, K.; Tanzi, R. E.; Masters, C. L. Metal-
688 Protein Attenuation with Iodochlorhydroxyquin (Clioquinol) Target-
689 ing $\text{A}\beta$ Amyloid Deposition and Toxicity in Alzheimer Disease: A
690 Pilot Phase 2 Clinical Trial. *Arch. Neurol.* **2003**, *60* (12), 1685–1691.
- (45) Mao, X.; Schimmer, A. D. The Toxicology of Clioquinol.
691 *Toxicol. Lett.* **2008**, *182* (1–3), 1–6.
- (46) Faux, N. G.; Ritchie, C. W.; Gunn, A.; Rembach, A.; Tsatsanis,
692 A.; Bedo, J.; Harrison, J.; Lannfelt, L.; Blennow, K.; Zetterberg, H.;
693 Ingelsson, M.; Masters, C. L.; Tanzi, R. E.; Cummings, J. L.; Herd, C.
694 M.; Bush, A. I. PBT2 Rapidly Improves Cognition in Alzheimer's
695 Disease: Additional Phase II Analyses. *J. Alzheimer's Dis.* **2010**, *20* (2),
696 509–516.
- (47) Lannfelt, L.; Blennow, K.; Zetterberg, H.; Batsman, S.; Ames,
697 D.; Harrison, J.; Masters, C. L.; Targum, S.; Bush, A. I.; Murdoch, R.;
698 Wilson, J.; Ritchie, C. W. Safety, Efficacy, and Biomarker Findings of
699 PBT2 in Targeting $\text{A}\beta$ as a Modifying Therapy for Alzheimer's
700 Disease: A Phase IIa, Double-Blind, Randomised, Placebo-Controlled
701 Trial. *Lancet Neurol.* **2008**, *7* (9), 779–786.
- (48) Nguyen, M.; Vendier, L.; Stigliani, J.-L.; Meunier, B.; Robert, A.
702 Structures of the Copper and Zinc Complexes of PBT2, a Chelating
703 Agent Evaluated as Potential Drug for Neurodegenerative Diseases.
704 *Eur. J. Inorg. Chem.* **2017**, *2017* (3), 600–608.
- (49) Mital, M.; Zawisza, I. A.; Wiloch, M. Z.; Wawrzyniak, U. E.;
705 Kenche, V.; Wróblewski, W.; Bal, W.; Drew, S. C. Copper Exchange
706 and Redox Activity of a Prototypical 8-Hydroxyquinoline: Implica-
707 tions for Therapeutic Chelation. *Inorg. Chem.* **2016**, *55* (15), 7317–
708 7319.
- (50) Nguyen, M.; Robert, A.; Sournia-Saquet, A.; Vendier, L.;
709 Meunier, B. Characterization of New Specific Copper Chelators as
710 Potential Drugs for the Treatment of Alzheimer's Disease. *Chem.* -
711 *Eur. J.* **2014**, *20* (22), 6771–6785.
- (51) Zhang, W.; Huang, D.; Huang, M.; Huang, J.; Wang, D.; Liu,
712 X.; Nguyen, M.; Vendier, L.; Mazères, S.; Robert, A.; Liu, Y.; Meunier,
713 B. Preparation of Tetradentate Copper Chelators as Potential Anti-
714 Alzheimer Agents. *ChemMedChem* **2018**, *13* (7), 684–704.
- (52) Zhao, J.; Shi, Q.; Tian, H.; Li, Y.; Liu, Y.; Xu, Z.; Robert, A.;
715 Liu, Q.; Meunier, B. TDMQ20, a Specific Copper Chelator, Reduces
716 Memory Impairments in Alzheimer's Disease Mouse Models. *ACS*
717 *Chem. Neurosci.* **2021**, *12* (1), 140–149.
- (53) Lakatos, A.; Zsigó, É.; Hollender, D.; Nagy, N. V.; Fülöp, L.;
718 Simon, D.; Bozsó, Z.; Kiss, T. Two Pyridine Derivatives as Potential
719 Cu(II) and Zn(II) Chelators in Therapy for Alzheimer's Disease.
720 *Dalton Trans.* **2010**, *39* (5), 1302–1315.
- (54) Pessoa, J. C.; Correia, I. Salan vs. Salen Metal Complexes in
721 Catalysis and Medicinal Applications: Virtues and Pitfalls. *Coord.*
722 *Chem. Rev.* **2019**, *388*, 227–247.
- (55) Storr, T.; Merkel, M.; Song-Zhao, G. X.; Scott, L. E.; Green, D.
723 E.; Bowen, M. L.; Thompson, K. H.; Patrick, B. O.; Schugar, H. J.;
724 Orvig, C. Synthesis, Characterization, and Metal Coordinating Ability
725 of Multifunctional Carbohydrate-Containing Compounds for Alz-
726 heimer's Therapy. *J. Am. Chem. Soc.* **2007**, *129* (23), 7453–7463.
- (56) Storr, T.; Scott, L. E.; Bowen, M. L.; Green, D. E.; Thompson,
727 K. H.; Schugar, H. J.; Orvig, C. Glycosylated Tetrahydroxalens as
728 Multifunctional Molecules for Alzheimer's Therapy. *Dalton Trans.*
729 **2009**, No. 16, 3034–3043.
- (57) Oliveri, V.; Vecchio, G. Prochelator Strategies for Site-Selective
730 Activation of Metal Chelators. *J. Inorg. Biochem.* **2016**, *162*, 31–43.
- (58) Noël, S.; Perez, F.; Pedersen, J. T.; Alies, B.; Ladeira, S.; Sayen,
731 S.; Guillon, E.; Gras, E.; Hureau, C. A New Water-Soluble Cu(II)
732 Chelator That Retrieves Cu from Cu(Amyloid- β) Species, Stops
733 Associated ROS Production and Prevents Cu(II)-Induced $\text{A}\beta$
734 Aggregation. *J. Inorg. Biochem.* **2012**, *117*, 322–325.

- 751 (59) Sampani, S. I.; Zdorichenko, V.; Danopoulou, M.; Leech, M.
752 C.; Lam, K.; Abdul-Sada, A.; Cox, B.; Tizzard, G. J.; Coles, S. J.;
753 Tsipis, A.; Kostakis, G. E. Shedding Light on the Use of Cu(II)-Salen
754 Complexes in the A3 Coupling Reaction. *Dalton Trans.* **2020**, *49* (2),
755 289–299.
- 756 (60) Gruenwedel, D. W. Multidentate Coordination Compounds.
757 Chelating Properties of Aliphatic Amines Containing α -Pyridyl
758 Residues and Other Aromatic Ring Systems as Donor Groups.
759 *Inorg. Chem.* **1968**, *7* (3), 495–501.
- 760 (61) Klement, R.; Stock, F.; Elias, H.; Paulus, H.; Pelikán, P.; Valko,
761 M.; Mazúr, M. Copper(II) Complexes with Derivatives of Salen and
762 Tetrahydro-salen: A Spectroscopic, Electrochemical and Structural
763 Study. *Polyhedron* **1999**, *18* (27), 3617–3628.
- 764 (62) Storr, T.; Merkel, M.; Song-Zhao, G. X.; Scott, L. E.; Green, D.
765 E.; Bowen, M. L.; Thompson, K. H.; Patrick, B. O.; Schugar, H. J.;
766 Orvig, C. Synthesis, Characterization, and Metal Coordinating Ability
767 of Multifunctional Carbohydrate-Containing Compounds for Alz-
768 heimer's Therapy. *J. Am. Chem. Soc.* **2007**, *129* (23), 7453–7463.
- 769 (63) Noël, S.; Bustos Rodriguez, S.; Sayen, S.; Guillon, E.; Faller, P.;
770 Hureau, C. Use of a New Water-Soluble Zn Sensor to Determine Zn
771 Affinity for the Amyloid- β Peptide and Relevant Mutants. *Metallomics*
772 **2014**, *6* (7), 1220–1222.
- 773 (64) Lovell, M. A.; Robertson, J. D.; Teesdale, W. J.; Campbell, J. L.;
774 Markesbery, W. R. Copper, Iron and Zinc in Alzheimer's Disease
775 Senile Plaques. *J. Neurol. Sci.* **1998**, *158* (1), 47–52.
- 776 (65) Atrián-Blasco, E.; Conte-Daban, A.; Hureau, C. Mutual
777 Interference of Cu and Zn Ions in Alzheimer's Disease: Perspectives
778 at the Molecular Level. *Dalton Trans.* **2017**, *46* (38), 12750–12759.
- 779 (66) Savelieff, M. G.; Nam, G.; Kang, J.; Lee, H. J.; Lee, M.; Lim, M.
780 H. Development of Multifunctional Molecules as Potential Ther-
781 apeutic Candidates for Alzheimer's Disease, Parkinson's Disease, and
782 Amyotrophic Lateral Sclerosis in the Last Decade. *Chem. Rev.* **2019**,
783 *119* (2), 1221–1322.
- 784 (67) Gal, S.; Zheng, H.; Fridkin, M.; Youdim, M. B. H. Novel
785 Multifunctional Neuroprotective Iron Chelator-Monoamine Oxidase
786 Inhibitor Drugs for Neurodegenerative Diseases. In Vivo Selective
787 Brain Monoamine Oxidase Inhibition and Prevention of MPTP-
788 Induced Striatal Dopamine Depletion. *J. Neurochem.* **2005**, *95* (1),
789 79–88.
- 790 (68) Zheng, H.; Fridkin, M.; Youdim, M. B. H. Site-Activated
791 Chelators Derived from Anti-Parkinson Drug Rasagiline as a Potential
792 Safer and More Effective Approach to the Treatment of Alzheimer's
793 Disease. *Neurochem. Res.* **2010**, *35* (12), 2117–2123.
- 794 (69) Shachar, D. B.; Kahana, N.; Kampel, V.; Warshawsky, A.;
795 Youdim, M. B.H. Neuroprotection by a Novel Brain Permeable Iron
796 Chelator, VK-28, against 6-Hydroxydopamine Lesion in Rats.
797 *Neuropharmacology* **2004**, *46* (2), 254–263.
- 798 (70) Gans, P.; Sabatini, A.; Vacca, A. SUPERQUAD: An Improved
799 General Program for Computation of Formation Constants from
800 Potentiometric Data. *J. Chem. Soc., Dalton Trans.* **1985**, No. 6, 1195–
801 1200.
- 802 (71) Alderighi, L.; Gans, P.; Ienco, A.; Peters, D.; Sabatini, A.; Vacca,
803 A. Hyperquad Simulation and Speciation (HySS): A Utility Program
804 for the Investigation of Equilibria Involving Soluble and Partially
805 Soluble Species. *Coord. Chem. Rev.* **1999**, *184*, 311–318.
- 806 (72) Daina, A.; Michielin, O.; Zoete, V. SwissADME: A Free Web
807 Tool to Evaluate Pharmacokinetics, Drug-Likeness and Medicinal
808 Chemistry Friendliness of Small Molecules. *Sci. Rep.* **2017**, *7* (1), 1–
809 13.
- 810 (73) Benet, L. Z.; Hosey, C. M.; Ursu, O.; Oprea, T. I. BDDCS, the
811 Rule of 5 and Drugability. *Adv. Drug Delivery Rev.* **2016**, *101*, 89–98.
- 812 (74) Matsson, P.; Kihlberg, J. How Big Is Too Big for Cell
813 Permeability? *J. Med. Chem.* **2017**, *60* (5), 1662–1664.
- 814 (75) Alies, B.; Renaglia, E.; Rózga, M.; Bal, W.; Faller, P.; Hureau, C.
815 Cu(II) Affinity for the Alzheimer's Peptide: Tyrosine Fluorescence
816 Studies Revisited. *Anal. Chem.* **2013**, *85* (3), 1501–1508.
- 817 (76) Streltsov, V. A.; Titmuss, S. J.; Epa, V. C.; Barnham, K. J.;
818 Masters, C. L.; Varghese, J. N. The Structure of the Amyloid- β
Peptide High-Affinity Copper II Binding Site in Alzheimer Disease. *1919*
Biophys. J. **2008**, *95* (7), 3447–3456. 820
- (77) Di Vaira, M.; Bazzicalupi, C.; Orioli, P.; Messori, L.; Bruni, B.;
821 Zatta, P. Clioquinol, a Drug for Alzheimer's Disease Specifically
822 Interfering with Brain Metal Metabolism: Structural Characterization
823 of Its Zinc(II) and Copper(II) Complexes. *Inorg. Chem.* **2004**, *43*
824 (13), 3795–3797. 825
- (78) Budimir, A.; Humbert, N.; Elhabiri, M.; Osinska, I.; Biruš, M.;
826 Albrecht-Gary, A. M. Hydroxyquinoline Based Binders: Promising
827 Ligands for Chelotherapy? *J. Inorg. Biochem.* **2011**, *105* (3), 490–
828 496. 829
- (79) Oliveri, V.; Vecchio, G. 8-Hydroxyquinolines in Medicinal
830 Chemistry: A Structural Perspective. *Eur. J. Med. Chem.* **2016**, *120*,
831 252–274. 832
- (80) Heffron, T. P. Small Molecule Kinase Inhibitors for the
833 Treatment of Brain Cancer. *J. Med. Chem.* **2016**, *59* (22), 10030–
834 10066. 835
- (81) Zeng, Q.; Wang, J.; Cheng, Z.; Chen, K.; Johnström, P.; Varnäs,
836 K.; Li, D. Y.; Yang, Z. F.; Zhang, X. Discovery and Evaluation of
837 Clinical Candidate AZD3759, a Potent, Oral Active, Central Nervous
838 System-Penetrant, Epidermal Growth Factor Receptor Tyrosine
839 Kinase Inhibitor. *J. Med. Chem.* **2015**, *58* (20), 8200–8215. 840
- (82) Halcrow, M. A. Jahn-Teller Distortions in Transition Metal
841 Compounds, and Their Importance in Functional Molecular and
842 Inorganic Materials. *Chem. Soc. Rev.* **2013**, *42* (4), 1784–1795. 843
- (83) Esmieu, C.; Balderama-Martínez-Sotomayor, R.; Conte-
844 Daban, A.; Iranzo, O.; Hureau, C. Unexpected Trends in Copper
845 Removal from A β Peptide: When Less Ligand Is Better and Zn Helps.
846 *Inorg. Chem.* **2021**, *60* (2), 1248–1256. 847
- (84) Csire, G.; Nagy, L.; Várnagy, K.; Kállay, C. Copper(II)
848 Interaction with the Human Prion 103–112 Fragment -Coordination
849 and Oxidation. *J. Inorg. Biochem.* **2017**, *170*, 195–201. 850
- (85) Aeschbach, R.; Amadó, R.; Neukom, H. Formation of
851 Dityrosine Cross-Links in Proteins by Oxidation of Tyrosine
852 Residues. *Biochim. Biophys. Acta, Protein Struct.* **1976**, *439* (2),
853 292–301. 854
- (86) Atwood, C. S.; Perry, G.; Zeng, H.; Kato, Y.; Jones, W. D.;
855 Ling, K. Q.; Huang, X.; Moir, R. D.; Wang, D.; Sayre, L. M.; Smith,
856 M. A.; Chen, S. G.; Bush, A. I. Copper Mediates Dityrosine Cross-
857 Linking of Alzheimer's Amyloid- β . *Biochemistry* **2004**, *43* (2), 560–
858 568. 859
- (87) Al-Hilaly, Y. K.; Williams, T. L.; Stewart-Parker, M.; Ford, L.;
860 Skaria, E.; Cole, M.; Bucher, W. G.; Morris, K. L.; Sada, A. A.;
861 Thorpe, J. R.; Serpell, L. C. A Central Role for Dityrosine
862 Crosslinking of Amyloid- β in Alzheimer's Disease. *Acta Neuropathol.*
863 *Commun.* **2013**, *1* (1), 83. 864
- (88) Maina, M. B.; Burra, G.; Al-Hilaly, Y. K.; Mengham, K.;
865 Fennell, K.; Serpell, L. C. Metal-and UV-Catalyzed Oxidation Results
866 in Trapped Amyloid- β Intermediates Revealing That Self-Assembly Is
867 Required for A β -Induced Cytotoxicity. *iScience* **2020**, *23* (10),
868 101537. 869
- (89) Maina, M. B.; Al-Hilaly, Y. K.; Burra, G.; Rickard, J. E.;
870 Harrington, C. R.; Wischik, C. M.; Serpell, L. C. Oxidative Stress
871 Conditions Result in Trapping of PHF-Core Tau (297–391)
872 Intermediates. *Cells* **2021**, *10*, 703. 873
- (90) Soragni, A.; Zambelli, B.; Mukrasch, M. D.; Biernat, J.;
874 Jeganathan, S.; Griesinger, C.; Ciurli, S.; Mandelkow, E.;
875 Zweckstetter, M. Structural Characterization of Binding of Cu(II)
876 to Tau Protein. *Biochemistry* **2008**, *47* (41), 10841–10851. 877
- (91) Zubčić, K.; Hof, P. R.; Šimić, G.; Jazvinščak Jembrek, M. The
878 Role of Copper in Tau-Related Pathology in Alzheimer's Disease.
879 *Front. Mol. Neurosci.* **2020**, *13*, 174. 880
- (92) Al-Hilaly, Y. K.; Pollack, S. J.; Vadukul, D. M.; Citossi, F.;
881 Rickard, J. E.; Simpson, M.; Storey, J. M. D.; Harrington, C. R.;
882 Wischik, C. M.; Serpell, L. C. Alzheimer's Disease-like Paired Helical
883 Filament Assembly from Truncated Tau Protein Is Independent of
884 Disulfide Crosslinking. *J. Mol. Biol.* **2017**, *429* (23), 3650–3665. 885